The vertical diffusivity and mean velocity of particles in a horizontal water pipe

By B. J. S. BARNARD AND A. M. BINNIE
Engineering Laboratory, Cambridge

(Received 20 July 1962)

Small spheres of the same size but of relative density varying from 0·92 to 1·25 were injected in turn into a horizontal water pipe, in which the flow was turbulent and the mean velocity was constant. A cross-section near the outlet was illuminated; the positions of the spheres as they crossed it were measured by photography, and the relation was established between the terminal velocity of the spheres in water and the vertical diffusivity. The velocity of the spheres along the pipe was found to be somewhat different in the galvanized steel and Perspex lengths of which the pipe was composed. The dispersion of the times of transit of the spheres increased slightly with their density. For purposes of comparison the theoretical velocity along the pipe was also calculated from the photographic measurements.

1. Introduction

Earlier papers in this series (Batchelor, Binnie & Phillips, 1955; Binnie & Phillips, 1958) have been concerned with the mean velocity of small spheres carried along in a horizontal water pipe. In the first the spheres were of neutral density, and in the second they were slightly buoyant or heavy. The experiments have now been extended to include spheres so heavy that they were frequently in contact with the bottom of the pipe, and an account is given below of timing measurements at three cross-sections of the pipe made in the same way as before. A few rather light spheres were also tried to test the symmetry of the results. The previous investigations showed that the mean velocity of the spheres was slightly greater than the discharge velocity, defined as the discharge, averaged over a long time, divided by the cross-section of the pipe. The discrepancy arose because the spheres, being of finite size, could not become immersed in the retarded layer near the wall. Now a markedly heavy or buoyant sphere may be expected to move more slowly than one of neutral buoyancy, and an object of the work was to examine the attractive possibility of finding a sphere that possessed a mean velocity exactly equal to the discharge velocity.

In addition, for the first time photographic observations were made of the positions of the spheres as they crossed a vertical section of the pipe, and an attempt has been made to relate the two sets of results. From the cross-sectional measurements the mean vertical diffusivity has been calculated by means of an approximate theory, the validity of which was tested.

2. Description of apparatus

A number of changes were made in the existing 2 in. pipe-line, some as the result of experience and others to accommodate the photographic equipment mentioned above. Three arrangements of the photocell detectors and of the galvanized steel and Perspex lengths in the 80 ft. straight require description; they are illustrated in figure 1.

(i) The sequence used by Binnie & Phillips consisted of a 30 ft. steel inlet length, a 1 ft. length of Perspex on which photocell A was mounted, two steel lengths S1 and S2 totalling 28 ft., two Perspex lengths P1 and P2 totalling 11 ft., a steel length S3 of 10 ft., and finally a 1 ft. Perspex length for the third photocell C. Photocell B was on P1, and the percentages of steel in AB and BC were 85 and 63.

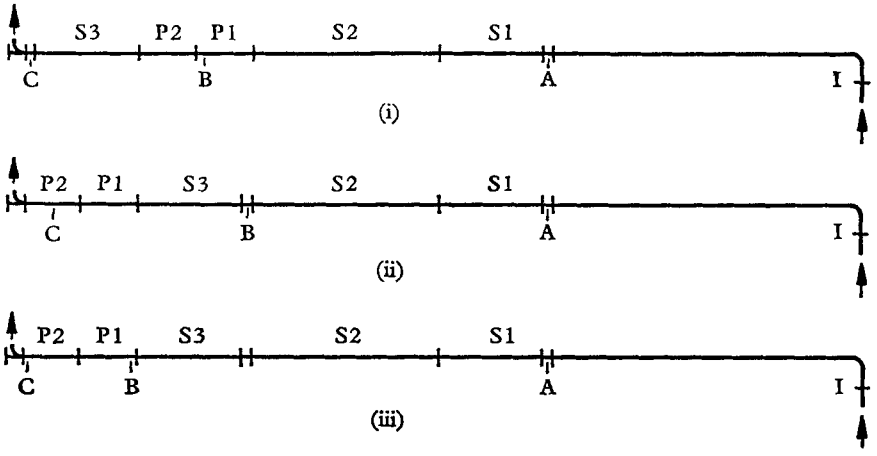

FIGURE 1. Plans of the three arrangements of piping. The spheres were injected at I.

(ii) As the cross-section to be photographed was necessarily close to the downstream end and would have been disturbed by discontinuities close to it on the upstream side, the last four components were rearranged in the order: a 1 ft. Perspex length (on which the photocell B was mounted), S3, P1 and P2, with C near the outlet of P2. Thus the photocells A and B measured the lapsed time over S1 and S2, and B and C over the composite length S3, P1, P2.

(iii) As will be described in § 3, it was discovered that the apparatus was sufficiently accurate to record the dependence of mean sphere velocity on the nature of the wall. Thereupon photocell B was moved to the entry of P1 so that the length AB was almost wholly of steel and BC wholly of Perspex.

The original counter was replaced by two separate Ericsson dekatron counters, started as before by photocell A and stopped respectively by B and C. An inverter was necessary to alter the pulses from the photocells into a form suitable for triggering the counters. This change increased the sensitivity of the photocells to such an extent that the direct-current supply to the 6 W bulbs and the valve filaments had to be obtained from accumulators. Again, one of the counters was used with two probes in the measuring tank to determine the discharge

velocity. The counters were operated off the 50 c/s mains; and no frequency correction was necessary because the absolute values of the discharge velocity and the mean velocity of the spheres were not required with great precision—only the ratio of these quantities.

At the downstream end of P 2 a 90° pitcher tee piece made of iron was attached, the flow through it being from line to branch and passing on to the measuring tank. The end of the straight part of the tee was blanked off by a glass window, through which photographs up the pipe were taken with a 35 mm camera. The lengths P 1 and P 2 were wrapped in black paper except for a slit, 17 in. from the window and $\frac{1}{8}$ in. wide, which was illuminated by three 150 W floodlights spaced at 120° round the pipe.

The automatic device for injecting the spheres was modified to operate three times a minute instead of four, as the spheres were now expected to move more slowly. The camera shutter was kept open while a number of spheres passed by, therefore a second disk with cams was attached to the shaft of the injector motor, and these engaged a micro-switch operating two relays so that the floodlights were switched on only for 4 sec during each cycle. As an additional precaution against fogging of the photographs, an auxiliary shutter was inserted in a tube between the window and the camera, and was controlled by a solenoid connected to the floodlight circuit.

The tee on which the injection apparatus was mounted was replaced by a cross, thus the apparatus could be fixed upside down when spheres much lighter than water were to be used. The concentric orifice-plate, further upstream, that controlled the discharge through the pipe, was not entirely satisfactory because from time to time the detectors were spuriously operated, possibly by a group of air bubbles that might have accumulated behind the plate. To remove this disturbance, an orifice-plate was used in the form of a circle with a segment at the top cut away. This gave a discharge velocity again about 5 ft./sec, depending slightly on the temperature. The corresponding Reynolds number based on pipe diameter was about 6×10^4.

Polythene spheres were used once more, all being of nominal diameter 0·2 in., thus the ratio α of sphere to pipe diameter remained 0·1. More batches with varying amounts of loading were kindly given to us by the Plastics Division of Imperial Chemical Industries Ltd. Their relative densities were in the range 0·92–1·25, and spheres of other densities were made by driving in short lengths of wire. When the terminal velocity V of the spheres in still water at the temperature of the tests was less than about 3 in./sec, it was measured directly in a long vertical tube. To sort the other spheres into batches while keeping their terminal velocity low and easily observed, the tube was filled with an alcohol–water mixture or a solution of common salt in water; then after the tests the density of the spheres was measured with a density-bottle in a constant-temperature room. This final step was later abandoned in favour of making up a solution in which the spheres neither sank nor floated, the density of the solution being then measured with the bottle. The corresponding values of V were calculated with the aid of the well-known empirical curve connecting the drag coefficient and the Reynolds number.

3. Preliminary experiments

A typical example of the photographs is reproduced as figure 2, plate 1. Tests with very heavy spheres decided which of the circular markings represented the circumference of the illuminated cross-section, and the foot of the vertical diameter is indicated by the arrows. Each negative was measured in a Hilger Universal Projector set to a magnification of ten. The values of the x and y co-ordinates of the centres of the spheres were found to be repeatable to 0·002 in. The number of spheres that could be successfully photographed on a single exposure varied from three to ten, depending on the whiteness of the particular spheres in use and on the increasing insensitivity of the film as the exposure time was lengthened. With very heavy or light spheres another factor was the likelihood of spheres eclipsing each other at the bottom or top of the cross-section.

The illuminated cross-section was 11 in. upstream from the pitcher tee, which was fitted in a horizontal plane, and any greater distance would have placed the camera too far away. It was therefore necessary to discover if the cross-section was influenced by the curved flow in the tee. A trial was made with 230 observations of spheres for which the ratio γ of terminal velocity V to discharge velocity U was only 0·0139. On another day, when γ had changed slightly to 0·0145 because the temperature had altered, 350 observations were obtained. The cross-sections on the photographs were divided into 10 pairs of vertical strips symmetrically disposed about the vertical diameter, and a count was made of the spheres in each strip. The χ^2 test for heterogeneity was applied by constructing $2 \times n$ tables in the manner due to Brandt & Snedecor which is explained in text-books, e.g. Mather (1943). The results for the two sets were $\chi^2 = 13{\cdot}3$ and 9·6; and for 9 degrees of freedom the corresponding probabilities are found from the table to be about 0·15 and 0·4. Thus there was no significant bias between the observations on the left and right sides of the vertical diameter, and the tee did not influence the flow at the illuminated cross-section.

Timing observations, varying in number from 198 to 375, were made at six different values of γ, and it was immediately noticeable that $U(\alpha, \gamma)$, the mean sphere velocity along the pipe, was greater in AB, which was all steel, than in BC, which was about half steel and half Perspex. The discordancies were too great to be explained by the small differences in the cross-sectional areas. Suspicion fell on the various electrical circuits, but this was dispelled by comprehensive tests. It was then realized that the effect was due to the slightly rougher surface of the steel pipe. In it, the velocity over the central part of the cross-section which was fully accessible to the spheres was greater, in order to compensate for the additional retardation near the walls. The effect had not been noticed by Binnie & Phillips as both their lengths AB and BC were composed of both materials. As mentioned in § 2, the photocells were moved to new positions such that AB was all steel except for an insignificant length and BC was all Perspex; and as the timing over AC was now of little interest, the dekatrons were connected to measure directly the times over AB and BC. A trial with these positions showed greater discrepancies than before, thus confirming the above explanation.

4. Theoretical discussion

(i) *The mean vertical diffusivity* ζ

In the previous work an expression for ζ was derived on the assumption that $\gamma = V/U$ was small. The theory must now be modified to remove this restriction.

We define by p the probability density that the projection on a transverse plane of the centre of the sphere falls at any instant within a specified unit area in that plane. It is supposed again as an approximation that p is a function $p(Z)$ of the vertical position co-ordinate only. We therefore consider an element of unit breadth situated a distance Z above the pipe centre. Then, V being the terminal velocity of the spheres measured positively downwards, the probability

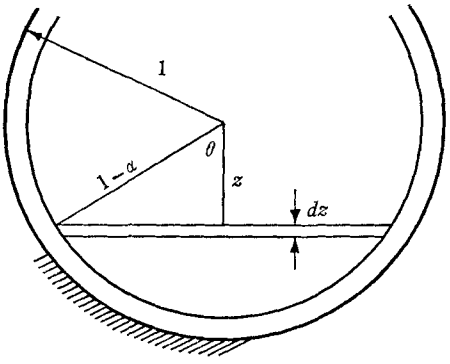

FIGURE 3. Cross-section of pipe.

of the sphere sinking in unit time across unit breadth of the horizontal plane defined by Z is

$$Vp(Z). \tag{1}$$

This must be balanced by the upward flux across the same area due to turbulent diffusion, which is

$$u_\tau a\zeta \frac{dp(Z)}{dZ}, \tag{2}$$

where u_τ is the friction velocity, a is the pipe radius, and ζ is the dimensionless turbulent diffusivity for transport across horizontal planes. As before, we shall neglect the variation in ζ with position and take it as the mean vertical diffusivity for turbulent flow in a pipe. It follows that

$$\frac{dp(Z)}{dZ} = \frac{V}{u_\tau a\zeta} p(Z), \tag{3}$$

hence

$$p(z) = p_0 \exp(Mz), \tag{4}$$

where

$$z = Z/a \quad \text{and} \quad M = \gamma U/u_\tau \zeta. \tag{5}$$

Equation (3) agrees with the expressions given by O'Brien (1933), Rouse (1939) and Vanoni (1946) for the vertical distribution of sediment in a watercourse. It is not invalidated by collisions with the wall, for the frequencies of sinking and rebounding across a horizontal plane near the wall are equal over a short time interval that includes the instant of impact. The constant of integration

p_0 is determined by the condition that $p(z)$ integrated over the circle of radius $1-\alpha$ accessible to the centre of the sphere must equal unity. With the notation indicated in figure 3, it appears that

$$z = (1-\alpha)\cos\theta, \tag{6}$$

hence
$$1 = -\int_0^{\pi} p_0 \exp\{M(1-\alpha)\cos\theta\}\, 2(1-\alpha)^2 \sin^2\theta\, d\theta, \tag{7}$$

and
$$p_0 = \frac{1}{2\pi(1-\alpha)^2} \frac{(1-\alpha)M}{I_1\{(1-\alpha)M\}}. \tag{8}$$

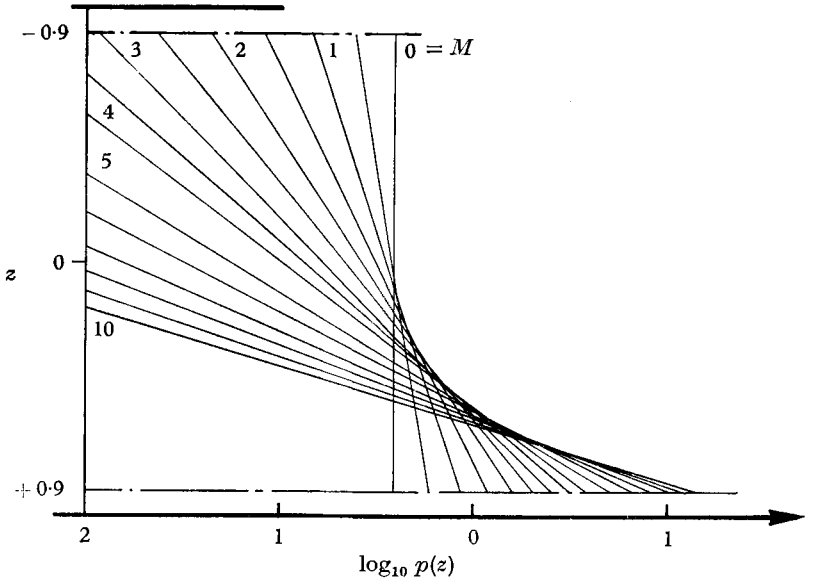

FIGURE 4. Theoretical distribution of the vertical probability density $p(z)$.

When $x \to 0$, $I_1(x)/x \to \frac{1}{2}$, therefore, for spheres of neutral density ($\gamma = 0$), (4) and (8) reduce to the expected result

$$p_0 = \frac{1}{\pi(1-\alpha)^2}. \tag{9}$$

Figure 4 displays the straight-line relationships between $\log_{10} p(z)$ and z for positive values of M (that is, for heavy spheres) within the range of the experiments. The lines for negative values of M are obtained by reflexion about the line $z = 0$.

(ii) *The relation between $p(z)$ and the mean velocity $U(\alpha, \gamma)$ of a sphere along the pipe*

We assume again that the mean velocity of the spheres whose centres are at radius R is equal to the mean velocity $u(R)$ of the fluid at radius R. Taking $Z = R\cos\theta$ and $r = R/a = z/\cos\theta$, we see with the aid of figure 3 that the mean velocity of a sphere down the pipe is given by

$$U(\alpha, \gamma) = 2\int_0^{\pi} \int_0^{1-\alpha} p(z)\, r u(r)\, dr\, d\theta. \tag{10}$$

On substituting (4) into (10) we obtain

$$U(\alpha,\gamma) = 2\pi p_0 \int_0^{1-\alpha} I_0(Mr)\, ru(r)\, dr. \tag{11}$$

It was shown by Taylor (1954) that $u(r)$ is given by

$$u(r) = U + 4{\cdot}25u_\tau - u_\tau f(r), \tag{12}$$

where $f(r)$ is a universal function. Then (11) becomes

$$U(\alpha,\gamma) = 2\pi p_0 \left[(U + 4{\cdot}25u_\tau)\frac{1-\alpha}{M} I_1\{(1-\alpha)M\} - u_\tau \int_0^{1-\alpha} I_0(Mr)\, rf(r)\, dr\right]. \tag{13}$$

For $\gamma = 0$, we find on using (9) that (13) reduces to

$$U(\alpha,\gamma) = U + 4{\cdot}25u_\tau - \frac{2u_\tau}{(1-\alpha)^2}\int_0^{1-\alpha} rf(r)\, dr. \tag{14}$$

The integral in (13) was evaluated numerically with the aid of the values of $f(r)$ given by Taylor, who also calculated the integral in (14).

(iii) *The relation between $p(z)$ and the photographic observations*

We consider the passage of the spheres across the fixed cross-section that was observed, and define by $P(z)$ the probability density of a sphere seen to be centred within a unit area distant z from the horizontal diameter. In view of the definition of $p(z)$ given at the beginning of § 4 (i) it appears that $P(z)$ is proportional to the product of $p(z)$ and the fluid velocity $u(z)$. Hence the relation between the two kinds of probability density is of the form

$$p(z) = C\frac{P(z)}{u(z)}, \tag{15}$$

where C is found from the condition that, as before, $p(z)$ summed over the accessible part of the cross-section must equal unity.

5. Experimental results

(i) *Friction loss*

The values of u_τ for the steel and the Perspex were required in many of the calculations, and they were determined by means of pressure tappings close to the photocells A, B and C in their final positions. The reading AB gave the friction loss in the steel length which was preceded by an ample inlet length, whereas for BC no inlet length could be arranged. Nothing seems to be known about the transition length required for the fully developed velocity profile to change after an abrupt alteration in the wall roughness. The friction coefficient for the Perspex length was found to be very slightly below the Blasius value for smooth pipes. The discrepancy can be attributed to the fact that at B the tapping was close to a joint, and in the calculations this part of the pipe was taken as smooth with $U/u_\tau = 20{\cdot}3$, derived from a logarithmic formula given by Goldstein (1938). For the steel the measured value $U/u_\tau = 18{\cdot}8$ was employed. Variations with temperature were inconsiderable.

(ii) *The probability density $p(z)$ and the diffusivity ζ in the Perspex pipe*

The illuminated cross-section was as much as 130 in. from the beginning of the Perspex pipe. This distance probably exceeded the transition length from steel to Perspex, and the observations can be regarded as made on the velocity distribution which is established in a smooth pipe.

The accessible part of the photographed cross-section was divided into horizontal strips with boundaries at $z = Z/a = 0, 0{\cdot}1, 0{\cdot}2, \ldots, 0{\cdot}8, 0{\cdot}84, 0{\cdot}86, 0{\cdot}88, 0{\cdot}9$, the width of the strips being reduced in that part of the cross-section where ζ

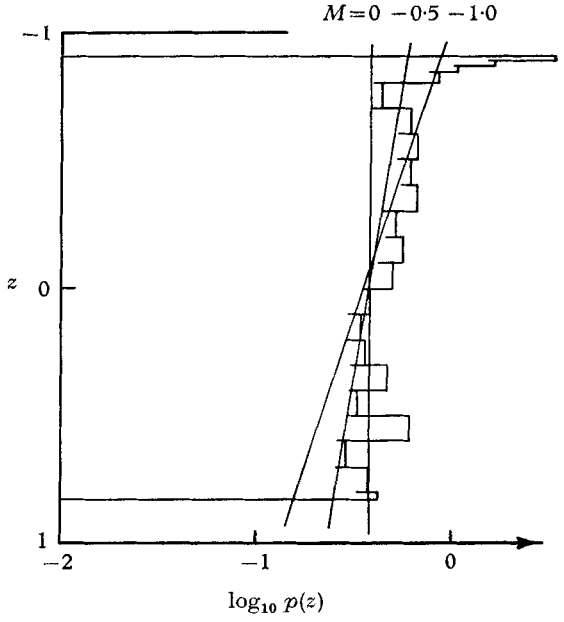

FIGURE 5. Measured distribution of the vertical probability density. $\gamma = -0{\cdot}027$.

was expected to change most rapidly. The number $n(z)$ of spheres centred in each strip of area, say, $A(z)$ was counted. Then $P(z)$ was given by

$$P(z) = n(z)/NA(z), \tag{16}$$

where N was the total number of spheres in the cross-section. It then follows from (15) that

$$p(z) = \frac{Cn(z)}{NA(z)\,u(z)}. \tag{17}$$

Here $u(z)$ is the mean fluid velocity over the strip. To evaluate it, the centre-line of each strip was divided into 20 elements of equal length, and the velocity at the mid-point of each element was calculated from the well-known formula

$$u(y)/u_\tau = 5{\cdot}5 + 5{\cdot}75 \log_{10}(u_\tau y/\nu), \tag{18}$$

where ν is the kinematic viscosity and $u(y)$ is the velocity at a point distant y from the wall. This expression is approximately valid over the turbulent core but not over the viscous sublayer and the buffer layer, for which Schlichting (1955) gave the limits $0 < u_\tau y/\nu < 5$ and $5 < u_\tau y/\nu < 70$. However, for spheres touching the wall $0 < u_\tau y/\nu < 170$–180, thus their motion was not greatly

influenced by these layers. The mean of the calculated velocities was taken as $u(z)$. The constant in (17) was determined by the condition

$$\Sigma p(z)\, A(z) = 1, \tag{19}$$

the summation including all the strips.

Two typical results are displayed in figures 5 and 6; the former is for fairly light spheres, and the latter is for the heaviest, which had a relative density 1·25.

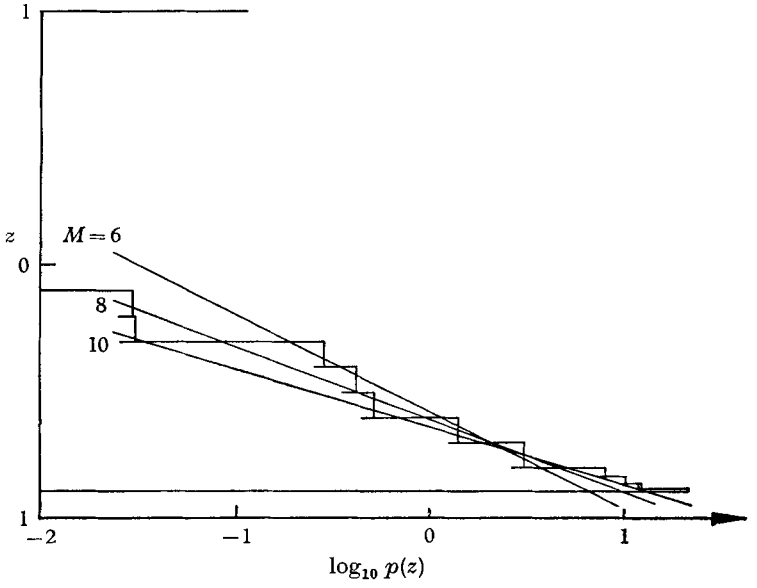

FIGURE 6. Measured distribution of the vertical probability density. $\gamma = 0{\cdot}118$.

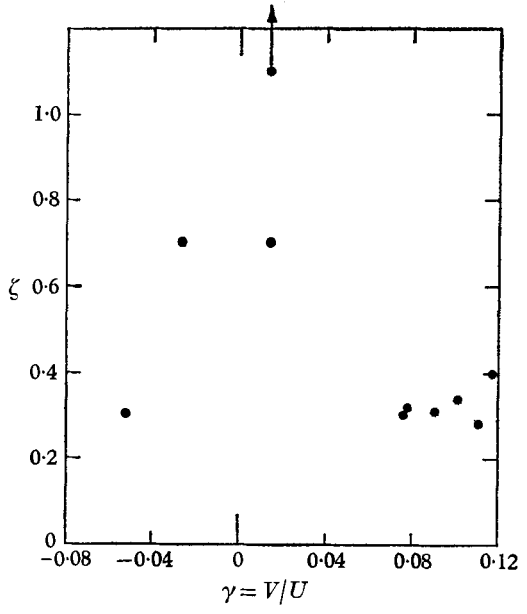

FIGURE 7. Effect of density upon the vertical diffusivity ζ.

Again the plotting is semi-logarithmic, so that the theoretical distribution lines transferred from figure 4 remain straight. The choice of M was matched as closely as possible to the experimental stepped distributions which generally followed one of the theoretical lines. Close to the wall, however, the distributions corresponded to progressively larger values of M. Thus ζ, as calculated from (5), was nearly constant over the central part of the cross-section, but declined towards the wall, where it may be expected to fall to zero.

For each batch of spheres ζ was estimated from diagrams like figures 5 and 6, and the results are plotted in figure 7. The approximate value of ζ was 0·3. It became larger for small values of $|\gamma|$, but the result was then sensitive to chance variations in the experimental distributions. For when M but not γ apparently almost vanished, ζ could become very great, and this happened in one of the tests.

(iii) *The mean velocity of the spheres*

(*a*) *In the steel pipe*

Figure 8 shows the mean values of $\mathscr{U}$, given by

$$\mathscr{U} = \{U(\alpha, \gamma) - U\}/U, \tag{20}$$

which were obtained by timing over lengths S 1 and S 2 in arrangement (ii), and over S 1, S 2, and S 3 in arrangement (iii). The total number of observations was 4019. The readings obtained by Binnie & Phillips with arrangement (i) were analysed with the transition length in BC taken as negligible. A small correction, depending on the relative lengths of steel and Perspex in AB and BC, was made to the observed times of transit in AB, which was mostly steel, and the results are included in figure 8. The diagram also contains three curves which give the theoretical relation between $\mathscr{U}$ and γ. They were calculated from (8) and (13) for $\zeta = 0{\cdot}4$, $0{\cdot}5$, $0{\cdot}6$ with the aid of the measured value of u_τ. The experimental values agree fairly well with the theoretical curve for $\zeta = 0{\cdot}5$. The discrepancy near $\gamma = 0$, where the theoretical estimate is somewhat too small, is not easy to explain. The theory supposes that the mean velocity of a sphere situated with its centre at r is the same as that of a fluid element at radius r. Thus the theory should overestimate $U(\alpha, \gamma)$, although by an amount shown in the previous work with neutral spheres to be very small for $\alpha = 0{\cdot}1$. For a sphere of this relative size the figure shows that the zero value of $\mathscr{U}$ was approximately attained at $\gamma = 0{\cdot}11$. At higher discharge velocities this result may be somewhat altered, because the experiments were carried out at a Reynolds number corresponding to turbulence nearly but not quite fully developed.

(*b*) *In the Perspex pipe*

Values of $\mathscr{U}$ obtained from 2492 timing measurements with arrangement (iii) are also given in figure 8 together with the theoretical curves for five values of ζ. At $\gamma = 0$ these curves differ from those for steel because the values of u_τ for the two materials were unequal. The experiments were not in the range where $\mathscr{U} = 0$, but the theoretical curves suggest that this result would have been reached at about $\gamma = 0{\cdot}05$, which differs substantially from the result with the steel pipe.

For purposes of comparison, estimates of $\mathscr{U}$ were made from the distributions shown in the photographs. It was thought that greater accuracy would result from the use of the radial rather than the vertical distribution. Accordingly the accessible cross-section was divided into rings with boundaries at $r = R/a = 0{\cdot}2$, $0{\cdot}4$, $0{\cdot}5$, ..., $0{\cdot}8$, $0{\cdot}84$, $0{\cdot}85$, ..., $0{\cdot}9$, and the numbers of spheres whose centres

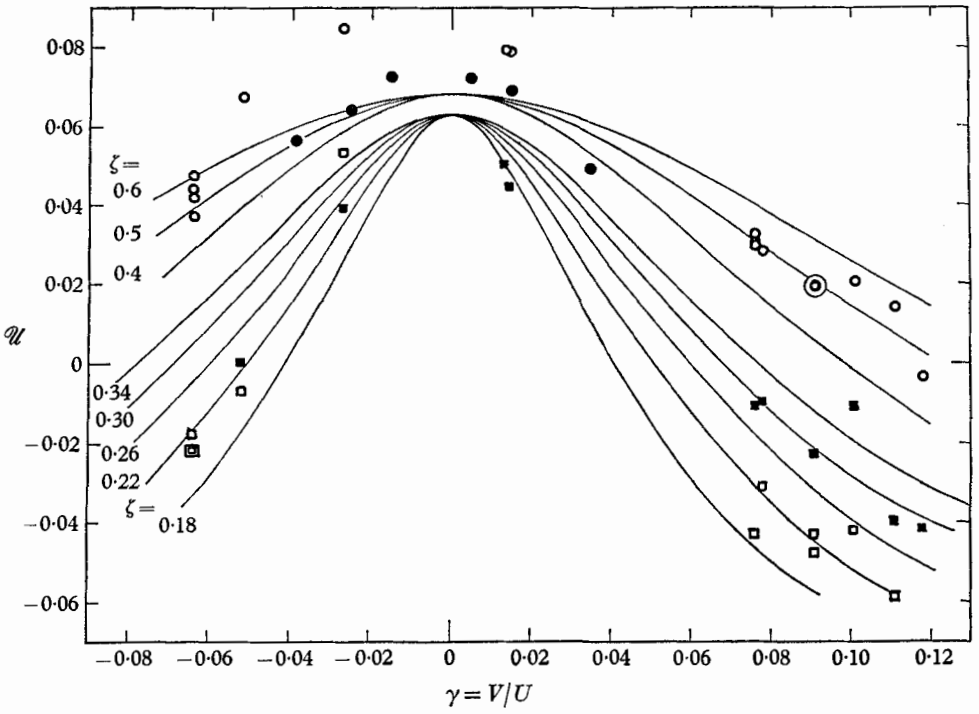

FIGURE 8. Effect of density upon $\mathscr{U} = \{U(\alpha, \gamma) - U\}/U$. ○, Steel, by timing spheres; ●, steel, estimated from Binnie & Phillips's timings; □, Perspex, by timing spheres; ■, Perspex, calculated from photographs.

fell within each ring were counted. Then, exactly as in § 4(iii) and 5(ii) but with r substituted for z, we have

$$p(r) = D\frac{P(r)}{u(r)}, \tag{21}$$

where $P(r)$ is found as in (16) and the constant D is determined as before from the summation condition. Again employing the principle on which (10) is based, we deduce that

$$U(\alpha, \gamma) = \Sigma p(r)\, A(r)\, u(r), \tag{22}$$

the summation including all the rings. Thus the mean velocity can be found after the insertion of the appropriate velocity over each ring of area $A(r)$. The simplest assumption is to take all the spheres centred within a ring to have the same velocity as the fluid at the mean radius of the ring. A more refined estimate, say $\bar{u}(r)$, is obtained if some allowance is made for the curvature of the mean velocity profile. Without serious error this can be done by direct integration if the contours of equal velocity over the profile of the sphere are taken as straight

instead of curved. Figure 9 shows two spheres drawn to scale, one near the centre and the other at the wall, with the two kinds of velocity distribution marked on them. Near the centre the discrepancy is considerable but the annular area is small; at the wall, where the annular area is large and where, moreover, heavy and light spheres are most likely to be found, the approximation is good.

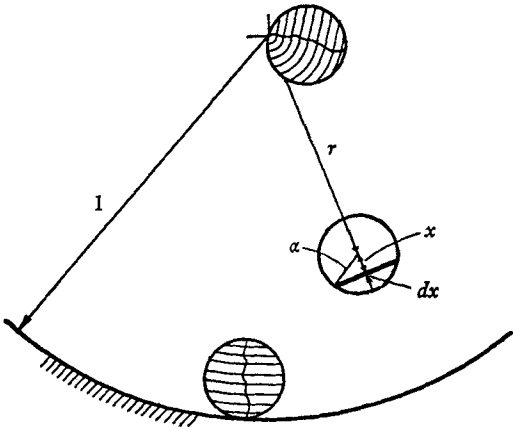

FIGURE 9. Cross-section of pipe and spheres.

We consider the profile, shown in figure 9, of radius α with its centre distant r from the pipe centre. The velocity over the element is taken as uniform and equal to that at radius $r+x$, which is given by the series expansion

$$u(r)+x\frac{du(r)}{dr}+\frac{x^2}{2!}\frac{d^2u(r)}{dr^2}+\ldots. \tag{23}$$

Hence the mean velocity over the profile of the sphere is

$$\begin{aligned}\bar{u}(r) &= \frac{1}{\pi\alpha^2}\int_{-\alpha}^{\alpha}\left\{u(r)+x\frac{du(r)}{dr}+\frac{x^2}{2!}\frac{d^2u(r)}{dr^2}+\ldots\right\}(\alpha^2-x^2)^{\frac{1}{2}}\,dx \\ &= u(r)+\frac{1}{4}\cdot\frac{\alpha^2}{2!}\frac{d^2u(r)}{dr^2}+\frac{1}{4}\cdot\frac{3}{6}\frac{\alpha^4}{4!}\cdot\frac{d^4u(r)}{dr^4}+\ldots. \end{aligned}\tag{24}$$

Then, with $u(r)$ determined from the logarithmic expression (18), the values of $\mathscr{U}$ plotted in figure 8 were calculated. They were somewhat greater than those obtained by timing, although the reverse was expected because of the transition length in BC. The correcting terms in (24) amounted to $0{\cdot}0215u(r)$ at $r = 0{\cdot}895$, ten terms in the expansion being required because near the wall, where the correction was important, the convergence of the series was very slow.

The results, repeating a less marked tendency among the steel experiments, were not quite symmetrical about $\gamma = 0$, and it is possible that this effect was due to the difference between the inertia of the spheres and that of the water they displaced. The theoretical curve $\zeta = 0{\cdot}26$ accords with many of the tests. Thus the value of ζ was now lower, for the smoother wall gave rise to a lesser intensity of the eddying motion of the water.

(iv) *The longitudinal dispersion coefficient* $K(\alpha, \gamma)$

The timing measurements yielded the values of this coefficient defined by Batchelor *et al.* as

$$K(\alpha, \gamma) = \frac{x}{2a} \frac{U}{u_\tau} \frac{\overline{[T(x) - \bar{T}(x)]^2}}{\bar{T}^2(x)}, \tag{25}$$

where $\bar{T}(x)$ is the average of the times $T(x)$ taken for a sphere to travel a distance x. As figure 10 shows, the scatter of the results is considerable, but they are in

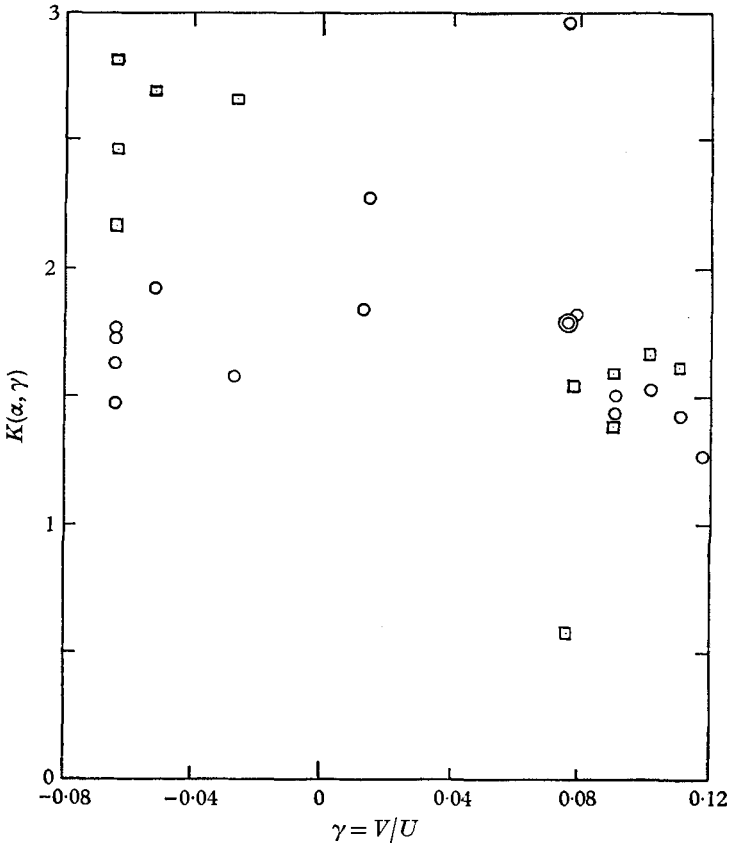

FIGURE 10. Effect of density on the longitudinal dispersion coefficient $K(\alpha, \gamma)$.
○, Steel; □, Perspex.

agreement with the previous work. There is a slight tendency for K to fall as γ increases. This again may be due to inertia effects, for we may expect that a heavy sphere will not entirely follow the movements of the surrounding liquid.

Histograms were drawn to show the distribution of the times of travel in the steel lengths, and Gaussian curves with standard deviations calculated from the observations were superposed. The agreement was satisfactory in accordance with the theory which holds good for all spheres transported in turbulent flow regardless of their density. The magnitude of the standard deviations did

not vary systematically with γ. For heavy spheres, for which γ was 0·111, the standard deviation was 0·127 sec over a distance 40·75 ft. This is much the same as Batchelor *et al.* obtained for neutral spheres. Their figure 7 gives standard deviations of 0·101 and 0·189 sec for distances 20·56 and 72·66 ft.

REFERENCES

BATCHELOR, G. K., BINNIE, A. M. & PHILLIPS, O. M. 1955 *Proc. Phys. Soc.* B, **68**, 1095.

BINNIE, A. M. & PHILLIPS, O. M. 1958 *J. Fluid Mech.* **4**, 87.

GOLDSTEIN, S. (Ed.) 1938 *Modern Developments in Fluid Mechanics*, p. 338. Oxford: Clarendon Press.

MATHER, K. 1943 *Statistical Analysis in Biology*, p. 198. London: Methuen.

O'BRIEN, M. P. 1933 *Trans. Amer. Geophys. Un.* **14**, 487.

ROUSE, H. 1939 *Proc. 5th Intern. Congr. Appl. Mech.* p. 550.

SCHLICHTING, H. 1955 *Boundary-Layer Theory*, p. 407. London: Pergamon.

TAYLOR, G. I. 1954 *Proc. Roy. Soc.* A, **223**, 446.

VANONI, V. A. 1946 *Trans. Amer. Soc. Civ. Engrs*, **111**, 67.

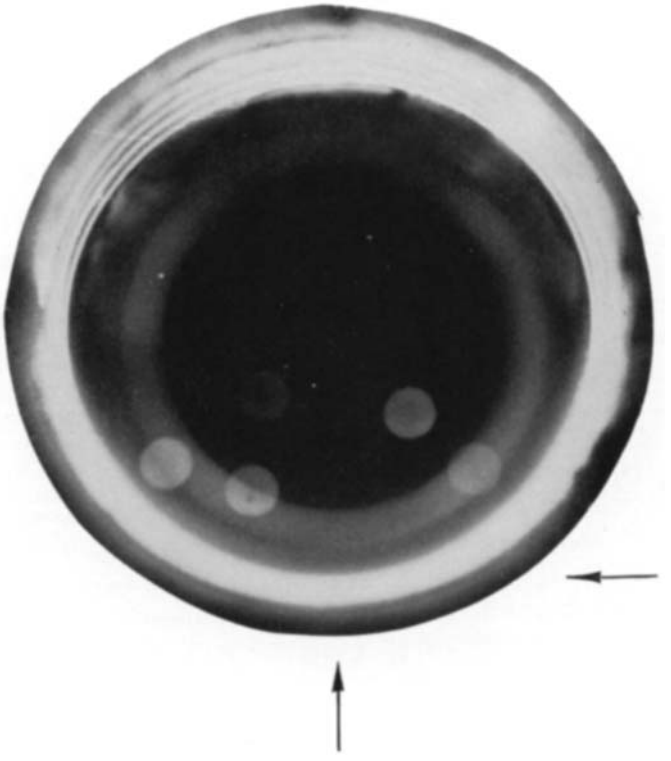

FIGURE 2. Photograph of cross-section.